Joint Deblending and Data Reconstruction With Focal Transformation

Cao, J.; Verschuur, D.J.; Gu, H.; Li, L

DOI
10.3997/2214-4609.201801533

Publication date
2018

Document Version
Final published version

Published in
80th EAGE Conference and Exhibition 2018, 11-14 June, Copenhagen, Denmark

Th P1 05

Joint Deblending and Data Reconstruction With Focal Transformation

J. Cao* (China University Of Geosciences), D.J. Verschuur (Delft University of Technology), H. Gu (China University Of Geosciences), L. Li (CNOOC)

Summary

Blended/simultaneous source shooting is becoming more widely used in seismic exploration and monitoring, which can provide significant uplift in terms of both acquisition quality and economic efficiency. Effective deblending techniques are essential in order to make use of existing processing and imaging methodologies. When dealing with coarse and/or irregularly sampled blended data, the aliasing noises of incomplete data will affect the deblending process and the crosstalk in the blended data will also have a bad influence on the process of data reconstruction. In this work, we propose a joint deblending and data reconstruction method using the double focal transformation to eliminate blending noise and aliasing noise in the coarse, blended data. Synthetic and numerically blended field data examples demonstrate the validity of its application for deblending and data reconstruction.

Introduction

Simultaneous source data acquisition offers many advantages over conventional acquisition, which could increase the source density in a low-cost manner and, thus, improves the quality of seismic data (Berkhout, 2008; Hampson et al., 2008). However, field obstacles and economic constraints in seismic acquisition often result in incomplete seismic field data. Therefore, reconstruction of the coarse and/or irregularly sampling data plays a fundamental role in the seismic data processing chain, to obtain aliasing-free, dense, and regularly sampled data for processing steps like 3D surface-related multiple elimination (SRME), wave equation-based migration, amplitude-versus-offset (AVO) analysis and time-lapse studies (Xu et al., 2010; Verschuur et al., 1992). A number of effective reconstruction methods can be divided in three categories: (1) Filter-based reconstruction, such as the usage of prediction error filters (Spitz, 1991); (2) Transformation-based reconstruction, such as Radon transformation (Trad, 2002); (3) Wave equation-based reconstruction, such as shot continuation (Spagnolini and Opreni, 1996). Combining the good features of transformation-based methods and wave equation-based methods, the double focal transformation is a very effective way to use prior knowledge for seismic data reconstruction (Kutscha and Verschuur, 2012).

But when dealing with blended data that is coarse and/or irregularly sampled, the aliasing noise of incomplete data will affect the deblending process and the crosstalk in the blended data will also hamper the process of data reconstruction. As a result, deblending alone or data reconstruction alone could not get satisfactory results. In this paper, we propose to use the focal transformation to connect the deblending and data reconstruction problems introduced by coarse and/or irregularly sampled blended data. The main motivation behind this connection is that deblending and data reconstruction solve similar sparsity-based inversion frames (see also Herrmann, 2010).

Deblending

We begin by first reviewing deblending using double focal transformation, which can be regarded as a sparse inversion problem of a blended dataset P_{bl} (Kontakis and Verschuur, 2014):

$$\min_{\substack{\delta\tilde{\mathbf{X}}_k \\ k=1,\dots,K}} \left\{ \sum_t \sum_{k=1}^{K} \left\| \delta\tilde{\mathbf{X}}_k \right\|_S \right\} \text{ s.t. } \sum_w \left\| \mathbf{P}_{\mathrm{bl}} - \sum_{k=1}^{K} \mathbf{W}_k^- \delta\mathbf{X}_k \mathbf{W}_k^+ \mathbf{\Gamma} \right\|_F \le \sigma \;\Rightarrow\; \mathbf{P}_{\mathrm{debl}} = \sum_{k=1}^{K} \mathbf{W}_k^- \delta\mathbf{X}_k \mathbf{W}_k^+ , \qquad (1)$$

and the deblended data $\mathbf{P}_{\mathrm{debl}}$ is recovered by calculating the adjoint double focal transform. Here K pairs of one-way extrapolation operators $\mathbf{W}_k^+$ and $\mathbf{W}_k^-$ are used. $\mathbf{W}_k^+$ extrapolates a wavefield from the surface to the *k*-th depth level z_k and the $\mathbf{W}_k^-$ does the reverse operation. $\delta\mathbf{X}_k$ is *k*-th focal subdomain in frequency-space. $\mathbf{\Gamma}$ is the blending operator that applies the blending code on the unblended data (Berkhout, 2008). σ represents the noise level. All variables or operators are in the frequency domain, except when marked with a hat symbol, in which case they are in the time domain. The notation $\|.\|_S$ and $\|.\|_F$ is used for the sum and Frobenius norm, respectively.

Data reconstruction

The coarse input data will lead to an ill-posed inversion problem. Using the $\boldsymbol{L_1}$ norm as the constraint on the focal subdomain, the total number of parameters to explain the data is reduced. This allows a better separation of signal and aliasing noise and, therefore, provides a better potential reconstruction (Kutscha and Verschuur, 2012). By adding a sampling operator $\mathbf{S}$ to the forward focal transformation, we minimize the data misfit only at the known measured traces and the equation for the multilevel focal reconstruction is formulated as

$$\min_{\substack{\delta\tilde{\mathbf{X}}_k \\ k=1,\dots,K}} \left\{ \sum_t \sum_{k=1}^{K} \left\| \delta\tilde{\mathbf{X}}_k \right\|_S \right\} \text{ s.t. } \sum_w \left\| \mathbf{P}_{\mathrm{us}} - \mathbf{S} \left\{ \sum_{k=1}^{K} \mathbf{W}_k^- \delta\mathbf{X}_k \mathbf{W}_k^+ \right\} \right\|_F \le \sigma \;\Rightarrow\; \mathbf{P}_{\mathrm{rec}} = \sum_{k=1}^{K} \mathbf{W}_k^- \delta\mathbf{X}_k \mathbf{W}_k^+ , \qquad (2)$$

where $\mathbf{P}_{\mathrm{us}}$ represents the input data at the available traces and reconstructed data $\mathbf{P}_{\mathrm{rec}}$ is calculated by transforming the estimated focal domain for any desired output sampling.

Joint deblending and data reconstruction

Looking into algorithm (1) and (2), we can find that deblending and data reconstruction are very similar underdetermined inversion problems. So when dealing with the coarsely sampled blended data, we can combine deblending and data reconstruction together with the following equation:

$$\min_{\substack{\delta\tilde{\mathbf{X}}_k \\ k=1,\ldots,K}} \left\{ \sum_t \sum_{k=1}^{K} \left\| \delta\tilde{\mathbf{X}}_k \right\|_S \right\} \text{ s.t. } \sum_w \left\| \mathbf{P}_{\text{bl,us}} - \left\langle \mathbf{S}\left\{ \sum_{k=1}^{K} \mathbf{W}_k^{-} \delta\mathbf{X}_k \mathbf{W}_k^{+} \right\} \right\rangle \mathbf{\Gamma} \right\|_F \le \sigma \Rightarrow \mathbf{P}_{\text{debl,rec}} = \sum_{k=1}^{K} \mathbf{W}_k^{-} \delta\mathbf{X}_k \mathbf{W}_k^{+} \ , \quad (3)$$

where $\mathbf{P}_{\text{debl,rec}}$ is the deblended and reconstructed data. Optimization problems of the form (1), (2) and (3) can be handled by solvers such as SPGL1 solver (van den Berg and Friedlander, 2008) or a faster greedy solver (Cao et al., 2017).

Examples 1: Synthetic data

An example of a coarsely sampled input synthetic shot gather is visualised in Fig. 1(a), where a sampling operator is applied and two out of three traces have been removed from the measurements. The coarse data is composed of three reflection events with hyperbolic moveout. The set of source locations are the same as the receiver locations. The total data consists of 101 shots with 34 traces per shot. Each trace has 256 samples with 4ms sampling interval. Due to the missing traces, the FK spectrum of the coarse data is strongly aliased in Fig. 1(e). As shown in the red circles (Fig. 1e), signal content and aliasing noise overlap, which makes them difficult to separate in the FK domain. To test algorithm (3), another blending operator $\mathbf{\Gamma}$ and its adjoint $\mathbf{\Gamma}^{\text{H}}$ are applied to the coarse data (Fig. 1a) and the pseudodeblended shot gather is shown in Fig. 1(b). The crosstalk noise (Fig. 1b) makes its FK spectrum (Fig. 1f) more complex when comparing it with Fig. 1(e). Looking at the focal subdomain with a 3-level focal operators in Fig. 2(a) and 2(b), the first reflection event is focused at the zero-time zero-offset point while the aliasing noise and/or crosstalk noise can't be represented by the focal operator, resulting in its spreading everywhere in the focal subdomain. The deblending and data reconstruction quality is evaluated using the following expression

$$Q = 10\log_{10}\left(\sum_w \left\| \mathbf{P}_{\text{ideal}} \right\|_F^2 \Big/ \sum_w \left\| \mathbf{P}_{\text{ideal}} - \mathbf{S}\{\mathbf{P}_{\text{debl,rec}}\} \right\|_F^2 \right), \quad (4)$$

where $\mathbf{P}_{\text{ideal}}$ is the unblended and properly sampled data. Please note that we calculate the Q only at the know measured traces. Additionally, we use a radial weights mask for the model space to make the signal energy more focused in the focal subdomain and allow a more flexible suppression of aliasing and crosstalk noise. After 400 spgl1 iterations, we get a very satisfactory deblended and reconstruction result with Q = 32.82 dB, as shown in Fig. 1(c). The error profile (Fig. 1d) is small enough to be ignored, which also applies to its FK spectrum in Fig. 1(h). In Fig. 2(c), we show that the aliasing and crosstalk noise are well supressed using the sparse inversion with the $\boldsymbol{L_1}$ norm constraint. The focal subdomain is sparse enough, and its FK spectrum (Fig. 1g) is demonstrating good separation and reconstruction.

Example 2: Numerically blended of a marine coarse field dataset

For our field data example, we test our algorithm on a subset of a 2D North Sea dataset, consisting of 151 sources. A sampling operator is applied to the input data with deleting two out of three receivers (Fig. 3a). Then, the extracted data is numerically blended with a blending factor of 2, as shown in Fig. 3(d). With the aid of joint deblending and reconstruction, and by applying the obtained sparse focal subdomain to the forward double focal transformation, we get good results with a Q value of 12.46 dB after 800 spgl1 inversion iterations (Figs. 3b and 3c). The differences at the known traces are small (Figs. 3e and 3f), indicating a successfully separation and reconstruction.

Conclusions

In this paper, we introduce a new optimization inversion algorithm for joint deblending and data reconstruction of blended data. Applications are illustrated using subsampled synthetic data and numerically blended marine field data, which demonstrate the validity of this algorithm. This method inspires a new way to simultaneous source acquisition, which allows us to significantly reduce the survey cost by using less measurements.

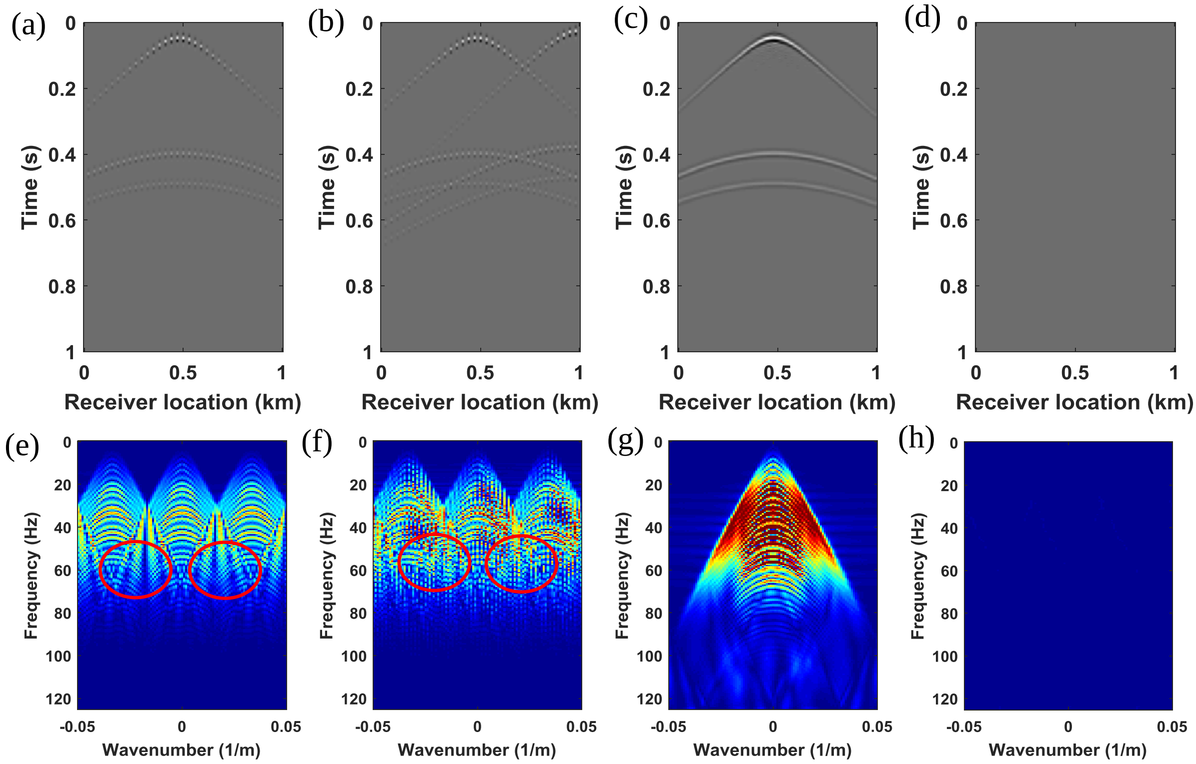

Figure 1 *Unblended, coarse shot gather in the space-time (a) and wavenumber-frequency domain (e). Blended shot gather of (a) in the space-time (b) and wavenumber-frequency domain (f). Deblended and reconstructed shot gather after 400 spgl1 iterations in the space-time (c) and wavenumber-frequency domain (g),(Q=32.82 dB). The difference between the Figure 1a and Figure 1c at the input known traces in the space-time (d) and wavenumber-frequency domain (h). The red circles denote areas where signal overlaps with noise (aliasing and /or crosstalk noise).*

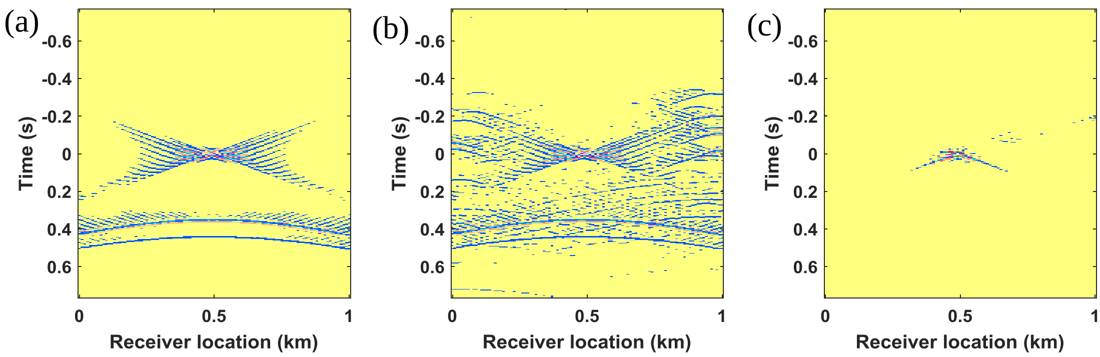

Figure 2 *(a) Focused shot gather from the coarse aliasing data in Figure 1a. (b) Focused shot gather from the blended data in Figure 1b. (c) Focused shot gather after 400 spgl1 iterations using sparse inversion.*

Acknowledgements

Junhai would like to thank the financial support of China Scholarship Council (CSC) and Delphi consortium sponsors, Statoil for providing the field data and Apostolos Kontakis for the stimulating discussions. This work is also funded by China National Major Science and Technology Projects (2016ZX05024-005-002).

References

Berkhout, A.J. [2008] Changing the mindset in seismic data acquisition. *The Leading Edge*, **27**(7), 924–938.

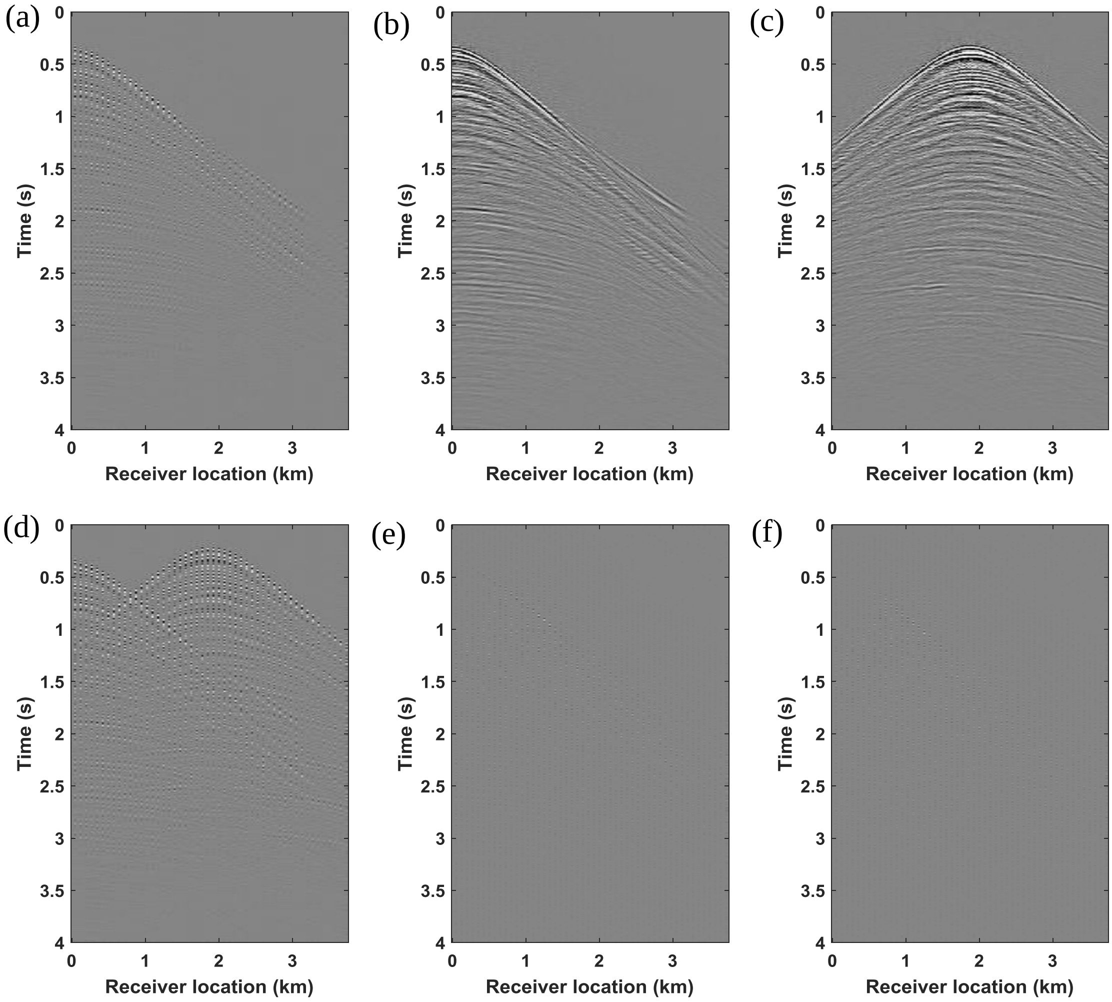

Figure 3 *Unblended, coarse shot gather (a) and blended shot gather (d). Deblended and reconstructed left shot gather (b) and right shot gather (c) after 800 spgl1 iterations (Q=12.46 dB). (e), (f) are the differences between Figure 3b, Figure 3c and the corresponding coarse input data at the known traces.*

Cao, J., Kontakis, A., Verschuur, D.J. and Gu, H. [2017]. Deblending using focal transformation with a greedy inversion solver. *79th EAGE Conference & Exhibition meeting*, Extended Abstracts, We P3 14.

Hampson, G., Stefani, J., and Herkenhoff, F. [2008]. Acquisition using simultaneous sources. *The Leading Edge*, **27**(7):918–923.

Herrmann, F.J.,[2010]. Randomized sampling and sparsity: Getting more information from fewer samples. *Geophysics*, **75**(6), WB173-WB187.

Kontakis, A., and Verschuur, D.J. [2014]. Deblending via a sparsity-constrained inversion in the focal domain. *76th EAGE Conference & Exhibition meeting*, Extended Abstracts, Th ELI2 02.

Kutscha, H. and Verschuur, D.J. [2012]. Data reconstruction via sparse double focal transformation: An overview. *IEEE Signal Processing Magazine*, **29**(4), 53-60.

Spagnolini, U. and Opreni, S. [1996]. 3-D shot continuation operator. *66th Annual International Meeting, SEG*, Expanded Abstracts, 439-442.

Spitz, S. [1991]. Seismic trace interpolation in the FX domain. *Geophysics*, **56**(6), 785-794.

Trad, D.O., Ulrych, T.J. and Sacchi, M.D. [2002]. Accurate interpolation with high-resolution time-variant Radon transforms. *Geophysics*, **67**(2), 644-656.

Van Den Berg, E. and Friedlander, M.P. [2008]. Probing the Pareto frontier for basis pursuit solutions. *SIAM Journal on Scientific Computing*, **31**(2), 890-912.

Verschuur, D.J., Berkhout, A.J. and Wapenaar, C.P.A. [1992]. Adaptive surface-related multiple elimination: *Geophysics*, **57**(9), 1166– 1177.

Xu, S., Zhang, Y. and Lambaré, G. [2010]. Antileakage Fourier transform for seismic data regularization in higher dimensions. *Geophysics*, **75**(6), WB113-WB120.